Chemical Geology 447 (2016) 161–172

Contents lists available at ScienceDirect

Chemical Geology

journal homepage: www.elsevier.com/locate/chemgeo

Rates of halite dissolution in natural brines: Dead Sea solutions as a case study

Mariana Stiller *, Yoseph Yechieli, Ittai Gavrieli

Geological Survey of Israel, 30 Malkhe, Jerusalem 95501, Israel

ARTICLE INFO

Article history:
Received 18 May 2016
Received in revised form 25 September 2016
Accepted 15 October 2016
Available online 19 October 2016

Keywords:
Halite
Degree of saturation
Dissolution rate
Dead Sea

ABSTRACT

The rate of salt dissolution is an important factor in many natural processes including the formation of sinkholes along the western shores of the Dead Sea (DS). The formation of these sinkholes which appear during the last 20 years in ever increasing numbers (~7000), is attributed to salt dissolution in the subsurface, by saline groundwater. However the rate of salt dissolution in the subsurface, by DS brines diluted with groundwater, is not known and is the main purpose of this study. Whereas most previous experimental studies on halite dissolution rates were performed in pure NaCl solutions and in fresh water, this study focuses on natural DS brines. The chemical composition of the DS is complex and besides NaCl includes high concentrations of Br and of Mg, Ca, and K chlorides. The present study is a laboratory attempt to assess the dissolution rates of natural halite in dilutions of DS brines, 10% to 90% by volume, under stirring and under no stirring conditions. The dissolution rates have been estimated by first order kinetics in the stirred runs and by derivatives of power best fits in the unstirred runs. In quiescent conditions, at 10 min the dissolution rates exhibit a very close to linear, inverse relationship to the degree of dilution and ranged between 12.2 mg/cm^2 min in 10% DS and 1.4 mg/cm^2 min in 90% DS. With stirring, in dilutions of 50% DS, the dissolution rates were about twice larger than without stirring: at 10 min they were 13 mg/cm^2 min vs. 5.8 mg/cm^2 min, respectively. The dissolution rates in stirred runs of DS dilutions appear to be about threefold slower than those reported in pure NaCl solutions of similar salinity and in a quite similar experimental setup. This divergence emphasizes the importance of measuring halite dissolution rates in natural solutions. The measured dissolution rates, in both stirred and non stirred solutions, decrease exponentially as the degree of saturation vs. halite, DSH, becomes larger, i.e. as saturation is approached. The exponential decrease in non stirred solutions is much faster. The results of this study will enable future studies to determine the rate of sinkhole formation in the Dead Sea area and other locations where halite salt is dissolved.

1. Introduction

1.1. Halite dissolution and formation of sinkholes along the Dead Sea shores

Since the late 1980's sinkholes are appearing along the western coast of the Dead Sea, at an ever increasing rate. This phenomenon is related to the drastic drop of the Dead Sea level, over the past decades, which is accompanied by a decline of the groundwater-DS brine interface at the subsurface (Wachs et al., 2000; Abelson et al., 2006; Yechieli et al., 2006). The formation of sinkholes is attributed to dissolution of halite deposits at the subsurface. Salt layers in the subsurface that were previously in contact with saturated (or almost saturated) DS brines, became increasingly exposed to contact with much less saline groundwater (Yechieli et al., 2006). As the halite layers gradually dissolve, large voids are formed in the subsurface. A new sinkhole appears on the lake shore whenever the overlying, unconsolidated sediments above a void finally collapse. A recent study (Oz et al., 2016) attempted to reproduce in the lab, in a transparent sand tank, the natural processes of sinkhole creation by forming a freshwater-saline water (concentrated NaCl solutions) interface and bringing it in contact with subsurface halite blocks or salt grains. They succeeded to track processes that occur in the subsurface and to show the direct connection between salt dissolution and the subsidence of layers above, finally leading to sinkhole formation.

The 'sinkholes phenomenon' raises the questions: how fast does halite dissolve by contact with various salinities of natural solutions, specifically with various salinities encountered in groundwater, By knowing the dependence of the dissolution rate on the salinity of the groundwater, it might become possible to predict, given the available stratigraphical and hydrogeological data, the timing, location and extent of formation of the subsurface voids. The present study deals with the

* Corresponding author.
E-mail address: stiller@netvision.net.il (M. Stiller).

http://dx.doi.org/10.1016/j.chemgeo.2016.10.023
0009-2541/

dependence of halite dissolution rate on groundwater salinities from the Dead Sea area.

1.2. The Dead Sea brines

The DS brine was formed during evaporation of seawater which intruded into the DS rift during the Neogene and underwent precipitation of evaporate minerals, such as gypsum and halite and interaction with the surrounding rocks (Starinsky, 1974).

The present DS contains beside sodium chloride, high concentrations of bromide and magnesium, calcium and potassium chlorides, (Gavrieli, 1997), as well as relatively high concentrations of heavy metals (Stiller and Sigg, 1990; Herut et al., 1998). The chemical composition of major ions in the surface water of the Dead Sea in 2003 and 2004 are given in Table 1. The Na/Cl molar ratio in the DS at that time was about 0.22, while in pure NaCl solutions it is unity.

Since the last century the continuous diversion of fresh water inflows from the drainage basin of the DS, for domestic and agricultural purposes, caused a negative water balance for the lake (evaporation > inflows), resulting in a rapid decline of the DS lake level and a continued increase in the lake's salinity. The lake level of the DS is presently declining at a rate of about 1 m/year (Lensky et al., 2005; Gertman and Hecht, 2002; Gavrieli and Oren, 2004). The DS first achieved saturation with respect to halite in 1979 (Steinhorn, 1983). Since 1982, depending on surface brine temperature, salt has been almost continuously precipitating in-situ. The solubility of halite as a function of temperature in Dead Sea brines has been studied by Gavrieli et al. (1989). Halite is accumulating at the lake floor (Stiller et al., 1997; Gavrieli, 1997) at a rate of about 0.1 m/year (Lensky et al., 2005).

Two short episodes of about 3 years each, caused by the unusually rainy winters of 1979/1980 and 1991/1992, have however interrupted the continuous NaCl deposition (Stiller et al., 1984; Anati et al., 1995). The heavy rains produced flooding which diluted the upper DS layer and caused undersaturation with respect to NaCl. Dissolution of halite from shallow areas of the lake has been observed concomitant with the flooding in winter 1991/1992 (Beyth et al., 1998). The extent of this process could not be predicted, as data on the rate of halite dissolution in diluted Dead Sea brines were not yet available.

1.3. Previous studies on halite dissolution rates

Halite dissolution rates in synthetic, pure NaCl solutions have been studied by Durie and Jessen (1964a), Wagner (1949), Alkattan et al. (1997a, 1997b), Pilcher and Blumstein (2007), Zidane et al. (2014) and references therein. Durie and Jessen (1964a) found, theoretically and experimentally, that initial dissolution rates under convective flow conditions are determined by the water salinity, from about 0.12 to 0.025 cm^3/cm^2 sec $* 10^{-3}$ in solutions of 0 to 4 mol NaCl/l. Under turbulent flow conditions the rates increase several fold. Alkattan et al. (1997a) performed short dissolution runs (mostly 5 to 10 min) in the absence or presence of dissolved trace metals, with varying concentrations of NaCl solutions, at varying stirring speeds and at several temperatures. The initial average dissolution rates obtained by dividing the dissolved amount of NaCl by the run duration and by the exposed surface area were in the range of 3 to 70 mg/cm^2 min. An inverse, linear relationship between the dissolution rates and the NaCl concentrations of the solutions was found. In the presence of metals the rates decreased and the linear relationship was not maintained.

Dijk et al. (2002) studied flow and dissolution patterns in halite rock fractures with rough walls. Saturated NaCl solutions flowed through rock fractures at ~1 mm/sec while pulses of unsaturated NaCl solutions were introduced in between to induce dissolution of the fracture walls. NMRI measurements were carried out during the flow of the saturated solution to monitor the rate of expansion of the fractures. Without defining halite dissolution rates, it was concluded that the dissolution pattern is correlated to rock fracture morphology, flow structure and mineralogic composition of rock matrix. Weisbrod et al. (2012) studied the dissolution pattern of halite salt rocks in natural solutions, in 70% to 95% (by volume) dilutions of Dead Sea brines. Dissolution rates of halite have not been explicitly mentioned, but the emphasis of this study was on the size and shape of channel formation and expansion in rock salt brought in contact with diluted Dead Sea brines. Field et al. (2015) studied the geometry of cavity formation of five different halite rock lithologies caused by through flow of brine (240 g/l NaCl) and of diluted seawater (24 g/l). Their experiments showed that the halite microstructure influenced the geometry of the cavity formed by contact with the brine. In contrast, similar shaped cavities were formed by contact with the more dilute seawater solution.

With the exception of Weisbrod et al. (2012) and Field et al. (2015), all the studies mentioned above have been performed with synthetic NaCl solutions under constant stirring or constant flow conditions Dissolution rates caused by natural brines with a more complex chemical composition, which penetrate the subsurface in the field in quiescent conditions, have not yet been estimated. The present study investigates the dissolution kinetics of halite in under-saturated Dead Sea (DS) brines under static or dynamic conditions. This study has practical aspects since the dissolution of halite by diluted DS solutions in the DS subsurface is the direct cause for the development of sinkholes along the shores of the Dead Sea (Abelson et al., 2006, Avni et al., 2015).

2. Experimental procedures

The experiments were performed by inserting halite slices into diluted DS solutions (Fig. 1). Table 2 summarizes the 71 kinetic runs and the 16 saturation experiments that have been performed.

Table 1
Molal concentrations (mole/kg water) of major ions in the Dead Sea 2003–2004.

Dead Sea surface brine		
	June 2003 Molal	December 2004 Molal
Na	1.57	1.55
K	0.21	0.23
Ca	0.48	0.51
Mg	2.07	2.20
Sr	0.004	0.004
Cl	6.80	7.08
Br	0.073	0.076
SO_4	0.006	0.006
TDS (kg/m^3)	325.7	338.6
Density at 25 °C (kg/m^3)	1226.3	1238.6
Water activity	0.692	0.664

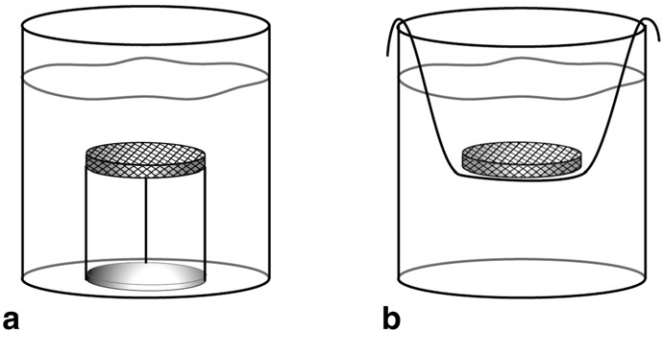

Fig. 1. (a) Schematic set up for runs with no stirring: halite slice suspended in solution by a three legged holder. (b) Schematic set up for runs with magnetic stirring: halite slice suspended in solution by a loose and large-holed cotton net.

Table 2
Experimental conditions and amounts of NaCl dissolved in diluted Dead Sea brines at 28 °C, measured by loss of halite from the immersed slice (W) and also by added Na (W_{Na}) and Cl (W_{Cl}) to solution. The degree of saturation vs. halite at end of each run is given in last column.

Run no.	Initial conditions				Duration of exp.	Final				Degree of saturation vs. Halite
	Density at 25 °C	Halite slice		Solution to slice area ratio		Density at 25 °C	NaCl	Dissolved		
		Weight	Total area				W slice	W_{Na} anal.	W_{Cl} anal.	
	g/cm³	g	cm²	cm³/cm²	min	g/cm³	g	g	g	DSH
Experiments with Dead Sea surface water sampled June 2003, density at 25 °C: 1.2263 g/cm³										
Runs with no stirring in 200 ml 10% Dead Sea										
M94	1.0220	14.132	28.71	6.97	9.5	1.0365	4.650	4.116	3.939	0.01
M95	1.0220	15.015	28.93	6.91	10.7	1.0430	6.030	6.152	6.009	0.01
M83	1.0220	17.833	30.15	6.63	18	1.0548	9.657	9.683	10.149	0.02
M84	1.0220	17.157	29.96	6.68	20	1.0540	9.622	9.760	9.618	
M87	1.0220	18.693	30.46	6.57	33	1.0667	14.004	13.552	13.688	0.03
M88	1.0220	22.997	31.62	6.33	46.5	1.0856	18.612	18.208	18.252	0.05
M89	1.0220	22.746	33.01	6.06	64	1.0879	20.672	20.567	19.901	0.06
M90	1.0220	27.381	35.04	5.71	71.3	1.0945	22.374	22.280	22.491	0.07
M132[a]	1.0230	37.554	41.31	4.84	90	1.1178	30.598	30.160	29.963	0.14
M133[a]	1.0230	38.814	41.72	4.79	100	1.1182	31.552	30.387	30.782	0.14
M92	1.0220	salt[b]	to saturation at 23 °C		14 days	1.1967	61.500	60.993	60.713	0.91
M93	1.0220	salt[b]	to saturation at 23 °C		14 days	1.2007	60.850	62.574	61.779	1.01
Runs with no stirring in 200 ml 50% Dead Sea										
M24	1.1167	14.884	28.88	6.93	20	1.1351	5.980	5.994	6.409	0.10
M25	1.1167	17.719	31.60	6.33	20	1.1307	4.540	4.654	5.399	0.09
M22	1.1167	16.395	29.15	6.86	40	1.1377	7.005	6.880	7.580	0.11
M23	1.1167	16.088	29.98	6.67	40	1.1393	7.415	7.573	8.383	0.12
M27	1.1167	17.616	30.83	6.49	70	1.1457	9.888	9.677	10.061	0.16
M28	1.1167	16.648	29.37	6.81	70	1.1439	9.103	9.092	9.160	0.15
M29	1.1167	19.768	31.20	6.41	110	1.1495	11.111	10.912	11.144	0.17
M30	1.1167	17.434	30.53	6.55	110	1.1514	11.835	11.741	12.482	0.19
M74	1.1164	13.640	26.27	7.61	146	1.1514	11.750	11.949	12.678	
M39	1.1169	3 slices			5 days	1.1997	29.788	29.147	29.983	0.71
M40	1.1169	3 slices	to saturation at 23 °C		15 days	1.2111	33.870	32.265	33.254	0.87
M48	1.1170	4 slices	to saturation at 23 °C		9 days	1.2104	32.118	33.353	33.944	0.94
M49	1.1170	salt[b]	to saturation at 23 °C		9 days	1.2105	33.010	33.664	34.893	0.99
M50	1.1170	4 slices	to saturation at 23 °C		9 days	1.2118	34.829	34.252	35.233	0.98
M51	1.1170	salt[b]	to saturation at 23 °C		9 days	1.2103	32.980	33.759	35.053	0.98
Runs with no stirring in 300 ml 50% Dead Sea										
M46	1.1167	14.460	28.60	10.49	61	1.1392	10.513	10.674	11.096	0.12
M47	1.1167	14.472	28.42	10.56	61	1.1366	9.323	9.034	9.533	0.10
M60	1.1161	16.968	30.01	10.00	90	1.1400	12.769	12.626	13.054	0.13
M59	1.1161	18.134	30.95	9.69	92	1.1428	13.045	13.100	13.273	0.13
M77	1.1164	19.080	31.09	9.65	155	1.1485	15.800	15.817	15.773	0.17
M76	1.1164	17.211	30.85	9.72	158	1.1480	15.283	15.192	15.782	0.16
Runs with no stirring in 800 ml 50% Dead Sea										
M79	1.1164	22.777	35.06	22.82	40	1.1280	9.914	14.782	11.499	0.08
M78	1.1164	21.866	32.22	24.83	41	1.1242	9.511	9.883	10.538	0.07
M110	1.1166	15.855	28.48	28.09	50	1.1249	10.494	12.007	5.524	0.07
M109	1.1166	15.471	28.58	27.99	61	1.1258	11.853	11.654	9.310	0.07
M72	1.1164	20.609	30.29	26.41	68	1.1249	13.737	11.310	13.226	
M73	1.1164	19.753	30.29	26.41	70	1.1249	13.133	11.289	14.056	0.08
M116[a]	1.1223	27.361	35.55	22.50	101	1.1395	21.473	21.691	20.138	0.10
M115[a]	1.1223	30.135	37.60	21.28	121	1.1384	24.018	19.889	19.908	0.10
Runs with no stirring in 200 ml 50% Dead Sea										
M66	1.1158	24.94	ground halite		35	1.1537	13.949	12.537	13.154	0.20
M65	1.1158	20.05	ground halite		73	1.1427	8.519	8.649	9.037	0.14
M64	1.1158	21.69	ground halite		104	1.1464	10.686	10.037	10.087	0.16
M63	1.1158	22.66	ground halite		135	1.1448	10.356	9.586	10.364	0.16
M62	1.1158	21.27	ground halite		165	1.1427	8.904	8.782	9.295	0.15
M68	1.1158	ground halite, saturation at 23 °C			18 days	1.2052	30.381	30.67	31.38	0.74
Runs performed with magnetic stirring, 350 rpm, at 23 °C in 200 ml 50% Dead Sea										
M112	1.1166	11.938	28.21	7.09	28	1.1438	9.218	8.398	8.446	0.14
M111	1.1166	12.430	27.46	7.28	30	1.1476	10.466	9.737	10.095	0.16
M113	1.1166	27.392	35.04	5.71	59	1.1660	17.243	19.825	16.981	0.34
M114	1.1166	26.902	35.49	5.64	75	1.1739	20.068	19.260	19.521	0.34
M127[a]	1.1231	29.990	36.62	5.46	90	1.1907	24.653	23.036	24.656	0.48
M128[a]	1.1231	33.378	38.72	5.17	106	1.1967	27.190	24.978	26.442	0.54
M129[a]	1.1231	39.288	41.20	4.85	121	1.2014	28.499	26.481	27.696	0.60
M130[a]	1.1231	40.240	42.00	4.76	137	1.1999	28.373	26.444	27.782	0.60
M135[a]	1.1235	42.453	42.80	4.67	235	1.2095	31.988	32.153	32.843	0.98

(continued on next page)

Table 2 (*continued*)

Run no.	Initial conditions				Duration of exp.	Final				Degree of saturation vs. Halite
	Density at 25 °C	Halite slice		Solution to slice area ratio		Density at 25 °C	NaCl	Dissolved		
		Weight	Total area				W slice	W_{Na} anal.	W_{Cl} anal.	
	g/cm^3	g	cm^2	cm^3/cm^2	min	g/cm^3	g	g	g	DSH
Runs with no stirring in 200 ml 70% Dead Sea										
LT23	1.1612	15.893	32.23	6.21	10	1.1646	0.780	0.790	0.361	0.16
LT24	1.1612	15.182	32.09	6.23	10	1.1654	1.075	1.158	0.944	0.17
M31	1.1612	11.710	28.00	7.14	22	1.1681	2.088	2.319	2.849	
M32	1.1612	14.882	28.77	6.95	22	1.1695	2.553	2.613	3.249	0.21
M33	1.1612	16.381	31.07	6.44	41	1.1718	3.392	3.361	3.185	0.22
M34	1.1612	16.047	29.84	6.70	41	1.1736	3.963	3.995	3.848	0.24
LT21	1.1612	13.772	31.22	6.41	60	1.1759	4.787	5.158	5.245	0.27
LT22	1.1612	13.228	32.09	6.23	60	1.1759	4.948	4.617	4.968	0.25
M35	1.1612	16.640	30.35	6.59	81	1.1784	5.726	6.028	5.843	0.29
M36	1.1612	19.104	31.37	6.38	81	1.1790	5.934	6.141	6.661	0.30
LT19	1.1612	13.778	31.08	6.44	136	1.1827	7.187	7.305	7.477	0.33
LT20	1.1612	14.493	32.23	6.21	136	1.1831	7.395	7.220	8.158	0.33
M81	1.1610	16.328	32.23	6.21	179	1.1841	8.171	8.180	9.552	0.35
M82	1.1610	13.701	31.94	6.26	180	1.1854	7.908	9.148	8.457	0.36
M41	1.1608	3 slices	to saturation at 23 °C		5 days	1.2119	18.493	18.732	20.051	0.83
M42	1.1608	3 slices	to saturation at 23 °C		5 days	1.2145	19.680	19.386	20.918	0.86
M52	1.1617	4 slices	to saturation at 23 °C		9 days	1.2182	20.905	20.239	19.516	0.82
M53	1.1617	salt[b]	to saturation at 23 °C		9 days	1.2178	18.800	19.935	19.011	0.82
M54	1.1617	salt[b]	to saturation at 23 °C		9 days	1.2176	18.550	20.606	22.055	0.94
M69	1.1624	ground halite, saturation at 23 °C			18 days	1.2172	n.m.	20.69	21.281	0.91
Runs with no stirring in 200 ml 90% Dead Sea										
M101	1.2053	15.102	27.98	7.15	182	1.2157	3.231	3.337	3.387	0.55
M102	1.2053	13.167	26.49	7.55	182	1.2161	3.299	3.773	4.753	0.63
M13	1.2046	12.408	26.14	7.65	240	n.m.	3.174	3.078	2.394	
M14	1.2046	14.153	26.95	7.42	240	n.m.	3.406	3.256	2.839	
M105	1.2053	15.112	30.35	6.59	442	1.2204	4.755	4.842	5.894	0.67
M106	1.2053	16.142	30.43	6.57	441	1.2203	4.430	4.408	4.648	0.62
M103	1.2053	18.117	29.82	6.71	1100	1.2207	5.747	5.809	6.119	0.70
M104	1.2053	17.466	30.01	6.66	1099	1.2215	5.763	5.652	6.071	0.69
M97	1.2053	20.854	31.60	6.33	1476	1.2217	5.890	5.956	6.086	0.68
M98	1.2053	19.093	32.82	6.09	1476	1.2234	6.344	6.444	6.599	0.74
M99	1.2053	salt[b]	to saturation at 23 °C		15 days	1.2289	6.655	8.460	8.334	0.88
M100	1.2053	salt[b]	to saturation at 23 °C		15 days	1.2287	6.928	9.123	8.619	0.94

[a] Run performed with Dead Sea surface water sampled Dec. 2004, density at 25 °C:1.2366 g/cm^3.
[b] Regular table salt, placed at beaker bottom.

2.1. Experimental set-up

2.1.1. Halite slices

Cores (3.7 cm dia.) were drilled in a consolidated rock salt block taken from Mount Sdom, a Neogenic salt diapir located on the western sea shore of the southern basin of the Dead Sea (Zak, 1967). The salt block was similar in appearance with halite blocks found in drillings near the sinkhole sites. The exterior of the drilled cores was fair grayish and quite homogenous. The cores were cut into slices ranging in thickness between 0.8 cm and 2.8 cm. The thicker slices were used in experiments with more diluted brines and in experiments of longer duration.

During the cutting the sliced surfaces gained a polished appearance. Based on the dimensions and weights of the slices, their average bulk density (n = 75) was 2.003 ± 0.104 g/cm^3 vs. 2.168 g/cm^3 for pure NaCl (www.mindat.org). The average weight of insoluble residue was 5.0 ± 2.9%. The small variations in bulk density and in insoluble residue concentrations (which include our analytical errors) attest for the homogeneity of the salt block. The insoluble residue was examined by XRD analysis and found to be built mostly of anhydrite (<5%) and some dolomite and calcite.

The initial weights and the initial total surface areas of the slices are given in Table 2. During the longer experiments, the slices lost some of their polished appearance. Dissolution experiments were also conducted with ground halite (2–4 mm) from the Mount Sdom cores and with fine grained commercial table salt.

2.1.2. Dilutions of Dead Sea brines

Surface DS brines, sampled in June 2003 and in December 2004, were diluted with distilled water to 10%, 50%, 70% and 90% (% volume DS). The densities and chemical compositions of the diluted DS brines were then measured (Stiller et al., 2007).

2.1.3. Dissolution runs with no stirring

48 runs (Table 2) were performed with 200 ml of diluted brine that was poured into a 250 ml pre-weighed beaker, which was then re-weighed. The beaker was placed in a thermostatic water bath at 28 °C (quiescent conditions, no shaking at all). A pre–weighed halite slice was placed on the legs of a plastic holder, which was introduced into the beaker with its legs upwards, thereby allowing the entire surface area of the slice to be exposed and in contact with the fluid (Fig. 1a). Experiments were repeated with 300 ml (6 runs) and 800 ml (8 runs) diluted brine in 400 ml and 1000 ml beakers, respectively. During the runs all beakers were covered with Parafilm. In runs with 200 ml and 300 ml diluted brine the slices were positioned at mid-height of the solution in the beaker. The 800 ml runs were performed with two holders, one on top of the other, at about 60% of the solution's height. At the end of each experiment, the holder + halite slice were withdrawn from the solution with a pair of tweezers. The halite slice was dried and weighed. The beaker with the solution was weighed. The solution was then filtered through a pre-weighed 0.45 μ membrane filter. The filter was dried and then weighed, to assess the amount of insoluble matter that

was released from the slice. The filtrate density was measured with a Paar density meter. The filtrate was diluted as required for analysis of major ions by ICP–AES (Optima 3300), for analysis of Cl + Br by titration with $AgNO_3$ and of Br by ICP-MS.

2.1.4. Dissolution runs with magnetic stirring

To achieve enhanced dissolution rate, 9 experiments were run with stirring, using a small magnet (length 3 cm, dia. 0.7 cm). The rock salt slice was placed in a loose cotton net rimmed to the top of a 250 ml beaker (Fig. 1b). The magnet and the net were pre-weighed together with the empty beaker. The height of the halite slice above the beaker floor was adjusted to be the same as in the *no-stirring* experiments. 200 ml diluted DS was poured into the beaker, which was then immediately placed on a magnetic stirrer plate, at 350 rpm. The temperature of the solution was about 22.5 °C at start and about 24.5 °C at the end of the run. The rest of the procedure was identical to the *no-stirring* experiments.

2.1.5. Experiments to approach halite saturation

Halite slices or ground halite or commercial, fine grained, table salt was left to dissolve in the dilutions of Dead Sea brine (10%, 50%, 70% and 90%, see Table 2). The beakers containing the halite with 200 ml diluted brine were tightly closed with Parafilm, to avoid evaporation losses during the long duration of these experiments (5 to 18 days) and placed in a thermostatic bath at 28 °C (Table 2). Occasionally during this period the beaker was shaken. The procedure at the end of the experiment was similar to that described above.

2.2. Calculations

To calculate the net weight, W, of NaCl (g) that was dissolved in a run, the weight of the slice at end of run and the weight of the insolubles (collected on the filter membrane) were subtracted from the initial weight of the slice.

The net weight of NaCl dissolved was also calculated from the chemical analyses and density measurements performed on the initial and final solution at the end of the run, as following:

$$W_{Na} = (((Na_{meas} - (Na_{init} * V_1/V_2)) * V_2)/(1000 * 1000)) * 58.5/23$$

$$W_{Cl} = (((Cl_{meas} - (Cl_{init} * V_1/V_2)) * V_2)/(1000 * 1000)) * 58.5/35.5$$

where: W_{Na} and W_{Cl} are the weights of dissolved NaCl (g) estimated independently from the Na and Cl analyses, respectively. Na_{meas} and Cl_{meas} are the respective concentrations (mg/l) at end of run and Na_{init} and Cl_{init} (mg/l) are the respective concentrations in the initial diluted brine. V_1 (ml) and V_2 (ml) are the initial and final volumes of the solutions, respectively.

V_1, the exact initial solution volume, was calculated by dividing the weight of diluted brine at run start by its density. The final solution volume V_2, is calculated from the initial weight of the solution plus the NaCl weight loss from the halite slice, divided by the density of the solution at run end.

The three independent estimates of the net weight of NaCl that was dissolved in a run, W, W_{Na} and W_{Cl} are mostly in good agreement with each other. The correlations between all W_{Na} and W and as well between all W_{Cl} and W were very good, $R^2 = 0.991$ in both cases.

V_2 is always larger than V_1 because the solution expands as it dissolves NaCl. The increase in volume, (V_2–V_1), is linearly related ($R^2 = 0.994$) to the amount of NaCl (W) that was dissolved (see Fig. 2a). Accordingly, each gram of NaCl dissolved in 1 l initial volume causes a volume increase of about 0.074 ml, or each mol of NaCl that is dissolved in 1 l cases a volume increase of 4.325 ml. Similarly, the density increase (corrected to 25 °C, g/cm^3) at the end of each run (Table 2), was found to be linearly related ($R^2 = 0.994$) to the amount of NaCl dissolved during the run (Fig. 2b): 0.00057 g/cm^3 per g NaCl/l or an increase in density by 0.0333 g/cm^3 for each mole NaCl dissolved in1 l. This correlation enables the calculation of the amount of NaCl dissolved in a run merely by measuring the initial and final densities of the experimental solution.

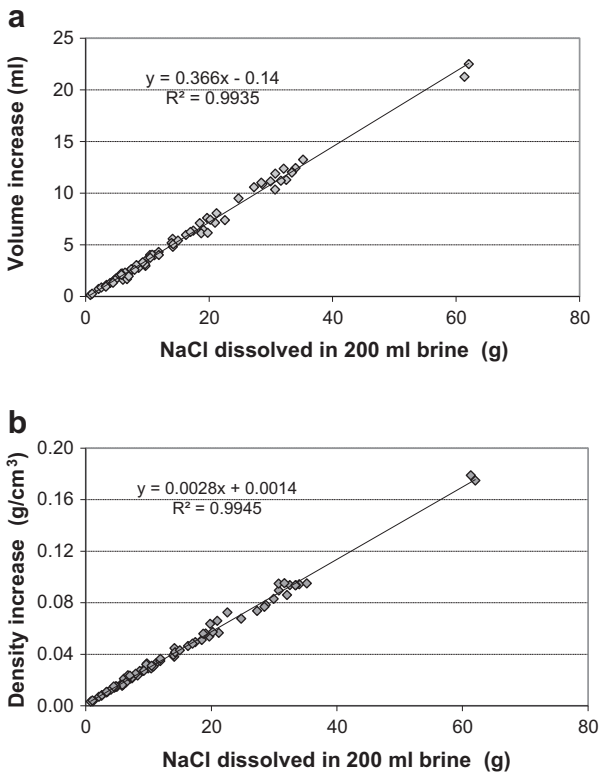

Fig. 2. (a) Increase in solution volume due to dissolution of NaCl. The correlation includes all the runs performed (initial volume 200 ml) at all different DS dilutions, and also the saturation experiments. (b) Increase in density at 25 °C due to dissolution of NaCl in 200 ml diluted brine. The figure includes all experiments (i.e. all DS dilutions). NaCl dissolved measured by loss of slice weight; W data were used.

The solutions' degree of saturation with respect to halite (DSH) at the end of each experiment was computed, with the complete chemical analyses of major ions in the filtrate at run end as the input parameters, by the open code PHREEQC (Parkhurst and Appelo, 2013) using Pitzer thermodynamic database and ion interaction equations embedded in the code (pitzer.dat).

3. Results

Table 2 summarizes the experimental conditions for all the experiments and the respective weights of NaCl that have been dissolved.

3.1. Dissolution of halite vs. time in 10%, 70%and 90% DS

Each data point in Fig. 3, as well as in all other figures, represents a separate experiment and shows the amount of halite dissolved by the end of the run. All the experiments with 10%, 70% and 90% DS (Fig. 3a,b,c) were run in 200 ml solution, with no stirring, at 28 °C. As expected the greatest amounts of halite were dissolved in 10% DS dilution and took place over a relatively short time (Fig. 3a), while the slowest and smallest dissolution was measured in 90% DS (Fig. 3c, note the different time scale for these runs). The duplicate runs of the latter series are in good agreement and in two cases are even undistinguishable from each other on the plot. Fig. 3a, b, and c show that the amount of dissolved NaCl does increase with run duration, but not linearly.

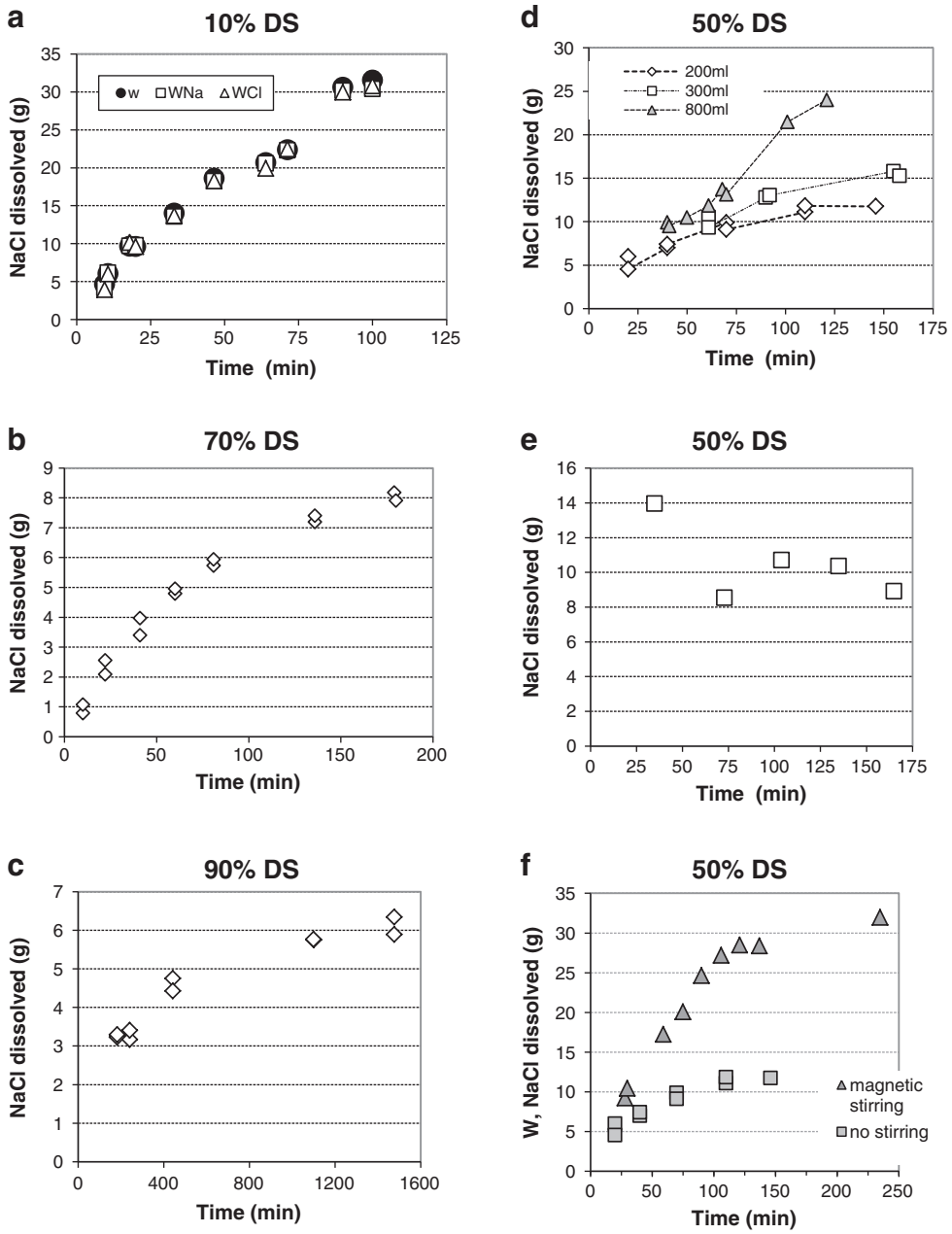

Fig. 3. NaCl dissolved from halite slices in 200 ml brine vs. duration of kinetic run: (a) in 10% DS, with no stirring using W (weight loss), W_{Na} and W_{Cl} (Na and Cl analyses) data - see Table 2. (b) In 70% DS with no stirring, based on W data. (c) In 90% DS with no stirring based on W data. (d) In 50%, no stirring, based on W data; also shown are runs performed in 300 ml and 800 ml. **(e)** ground halite immersed in 50% DS, no stirring. (f) In 50% DS, with magnetic stirring. Data with no stirring also shown, for comparison. The bars of the analytical error of the data points are too small to be seen on the figure.

3.2. Dissolution of halite vs. time in 50% DS

3.2.1. Halite slices with no stirring

Experiments with 50% DS and no stirring were conducted in 200 ml, 300 ml and 800 ml solution (Fig. 3d). Duplicates of the experiments are approximately within 10% reproducibility.

As also mentioned above, the weight of dissolved NaCl does not increase linearly with the duration of the experiment (Fig. 3d). Also, in the 300 ml and 800 ml runs, the increase in the ratio of solution volume to slice area (Table 2) does not cause a proportional increase in the amount of NaCl dissolved. Rather, it seems that during the first ~60 min of the runs the amounts of NaCl dissolved are about the same (Table 2 and Fig. 3d), irrespective of the volume (200, 300 or 800 ml). After that the increase in dissolved NaCl between 200 ml and larger volumes is significant mostly in the 800 ml runs.

3.2.2. Ground halite, no stirring

The 5 experiments with ground (millimeter sized grains) halite were performed with no stirring in 200 ml of 50% DS dilution (Fig. 3e; each data point represents the amount of dissolved halite at the end of the experiment). The weight of halite used in each of these experiments was about 22 g, similar to the weight of a single, medium sized halite slice. No clear trend in dissolution vs. time is observed with the ground halite and about the same amount of NaCl has been dissolved in most runs: 9.6 ± 1.1 g, $n = 4$. Exception to this is the shortest run in which a somewhat larger amount, 12.5 g, was dissolved (first data point in Fig. 3e). Thus, dissolution during the first 40 min takes place quite fast and shortly afterwards almost ceases. The amounts of ground halite dissolved in 50% DS dilutions are significantly larger than in runs in halite slices with similar 50% solutions (compare Fig. 3d and e), probably because of the much larger surface area of the ground halite. The

dissolution of halite leads to an increase in the solution's density. It is assumed here that the near ceasing of dissolution of the ground halite following the rapid, initial dissolution is due to the fact that the ground halite lied on the beaker's bottom and the layer of brine that formed with dissolved halite and increased density remained at the bottom too, allowed density stratification to develop just above it. In contrast, in the experiments in which the slices were suspended in the solution, stratification is was weakened by gravitational downward mixing, thereby making further dissolution possible.

3.2.3. Halite slices with stirring

Dissolution of halite rock slices with magnetic stirring in 200 ml 50% DS is more than twice larger than in runs with no stirring (Fig. 3f). Because of the anticipated larger dissolution, thicker slices were used in the longer duration experiments. As the thicker slices have larger surface areas, this resulted in different ratios of volume to slice area; ratios from about 7 (cm^3/cm^2) in the shorter duration runs to about 4.8 (cm^3/cm^2) in the longest ones (Table 2).

3.3. Experiments for attainment of halite saturation

The amounts of NaCl that have been dissolved in experiments designed to approach halite saturation at various DS dilutions are given in Table 2.

Table 3 compares these quantities with the weights of halite, calculated by the PHREEQC, that need to be dissolved in order to attain DSH = 1. Obviously, the higher the DSH attained in a run the better is the agreement between the measured and the calculated dissolved amounts (Table 3). Furthermore, there is a strong inverse linear correlation (see footnote in Table 3) between the degree of dilution of the DS brine and the amounts of NaCl that have been dissolved to approach saturation. This correlation enables without performing detailed chemical analysis and DSH calculations, an estimate of how much NaCl can be dissolved into any dilution of DS brine. For example, after winter floods, when the surface layer of the DS becomes diluted, it becomes possible to predict how much halite submerged in shallow areas can be dissolved.

4. Discussion - rates of halite dissolution

4.1. The rate of halite dissolution with magnetic stirring

Dissolution rates of halite in fresh water or pure NaCl solutions have been studied by numerous workers (e.g. Wagner, 1949; Durie and Jessen, 1964a, 1964b; Alkattan et al., 1997a, 1997b; Pilcher and Blumstein, 2007; Zidane et al., 2014 and references therein) under conditions of laminar or turbulent flow. Their empirical results have been interpreted by adequate mathematical models that fully described the experimental system. Dissolution rates of halite in diluted natural brines have not yet been measured. The scope of the present study is to examine and compare, in a simple experimental set-up, the influence of variable diluted DS brines on the dissolution rates of halite.

The set of experiments with stirring (runs M111-M114, M127-M131 and M135, Table 2) enabled assessment of the dissolution rate of halite in a well mixed environment, free of concentration gradients that may build up around the halite. In order to apply a first order kinetic model as usual, the disappearance of the reactant vs. time, i.e. the diminishing weight of the halite slice, should be followed. But in this set of runs, in which the initial weights of the slices are different from run to run, it was chosen to follow the gradual appearance of the product, i.e. the amounts of dissolved NaCl that have been added to the initial solution (which was always the same, 50%DS). Results from these experiments (Fig. 3f) suggest that the amount of dissolved NaCl added to the solution decreases with time, as saturation is approached. The rate of increasing dissolved NaCl concentration in solution (dC_t/dt), which is in fact equal to the dissolution rate of NaCl, can be treated as a first order reaction;

$$dC_t/dt = \lambda(C_{sat}-C_0)e^{-\lambda t} \quad (1)$$

where λ (min^{-1}): dissolution constant. C_0: initial concentration of Na in the DS dilution. C_{sat}: concentration of Na in the DS dilution at saturation with respect to NaCl. C_t: concentration of dissolved Na at time t ($C_t = C_0$ + amount of Na that has been added by NaCl dissolution by time t).

According to Eq. (1), the dissolution rate decreases exponentially with time. Integrating Eq. (1) yields:

$$C_t = -(C_{sat}-C_0)e^{-\lambda t} + C_{sat} \quad (2)$$

Rearranging Eq. (2)

$$C_{sat}-C_t = (C_{sat}-C_0)e^{-\lambda t} \quad (3)$$

And in logarithmic form

$$\ln(C_{sat}-C_t) = \ln(C_{sat}-C_0)-\lambda t \quad (4)$$

A plot of $\ln(C_{sat}-C_t)$ vs. time t, should be a straight line with slope λ and intercept $\ln(C_{sat}-C_0)$.

Fig. 4a presents the plots of $\ln(C_{sat}-C_t)$ vs. time t for halite dissolution runs with magnetic stirring, all with DS diluted to 50%. Note that runs M111-M114 and runs M127-M130 are plotted separately. This is because they were performed with DS surface water sampled at two different dates, June 2003 and December 2004, respectively, with the former being less saline than the brine collected in December 2004 (Tables 1 and 3). Accordingly, the dissolution potential (the amount of NaCl that must be dissolved to attain saturation) in the 50% DS of June 2003 is slightly higher than in 50% DS of December 2004 surface brine (Table 3, see measured amounts in columns 5 and 6 and also calculated ones in column 7).

The two sets of experiments yield linear plots (Fig. 4a) with very slightly different slopes (i.e. dissolution constants λ, Eq. (3)) and C_{sat} values. The calculated C_{sat} values from the intercepts in Fig. 4a indicate a somewhat higher C_{sat} in DS of June 2003.

The instantaneous dissolution rates (dC_t/dt) in these two sets of experiments were calculated by inserting the respective dissolution constants, λ, derived from the linear plots of Fig. 4a into Eq. (1). Fig. 4b plots the resulting values showing that the instantaneous dissolution rates decrease exponentially with time.

4.2. The rate of halite dissolution with no stirring

The weight loss of the halite slices, W, increases with duration of the *no stirring* runs (Fig. 3a,b,c,d) as do W_{Na} and W_{Cl} (shown together only

Table 3
Approach to saturation with respect to halite at various Dead Sea dilutions.

Run no.	Initial DS content[a] vol.%	Initial Na molality	Final Na molality	DSH attained	NaCl dissolved, based W_{Na}[b] molality	Calculated Na at DSH = 1 molality
Dead Sea surface brine sampled in June 2003; its density at 25 °C was 1.2263 g/cm^3						
M93	10	0.147	5.675	1.013	5.528	5.677
M49	50	0.736	3.816	0.986	3.080	3.890
M51	50	0.736	3.829	0.983	3.093	3.943
M54	70	1.046	2.952	0.936	1.907	3.047
M100	90	1.364	2.283	0.936	0.919	2.335
Dead Sea surface brine sampled in December 2004; its density at 25 °C was 1.2366 g/cm^3						
M135	50	0.739	3.684	0.980	2.945	3.832

[a] Densities at start and end of these runs are given in Table 2.
[b] Inverse linear correlation of W_{Na} (column 6) with initial DS content (column 2) is $R^2 = 0.998$.

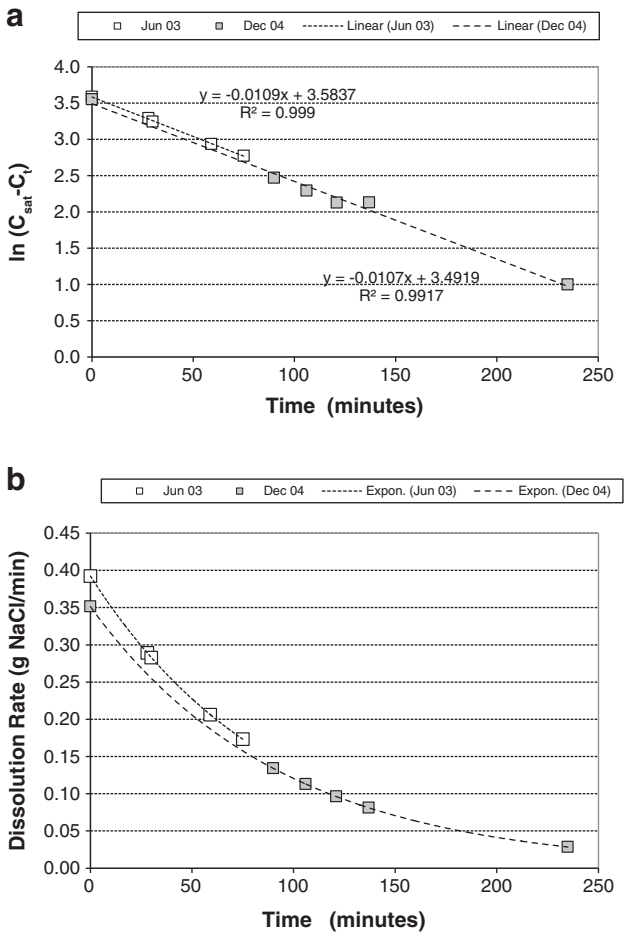

Fig. 4. (a) estimates of λ, the dissolution constant of NaCl, in 200 ml runs with magnetic stirring. $\lambda = 0.0109\ min^{-1}$ for runs M111-M114 (open squares, June 2003 50% DS) and $\lambda = 0.0107\ min^{-1}$ for runs M127-M130 and M135 (shaded squares, Dec. 2004 50% DS). (b) Momentary dissolution rates with magnetic stirring in 50% DS from June 2003 (open squares) and Dec. 2004 (shaded squares). The data points shown are at the end of each kinetic run.

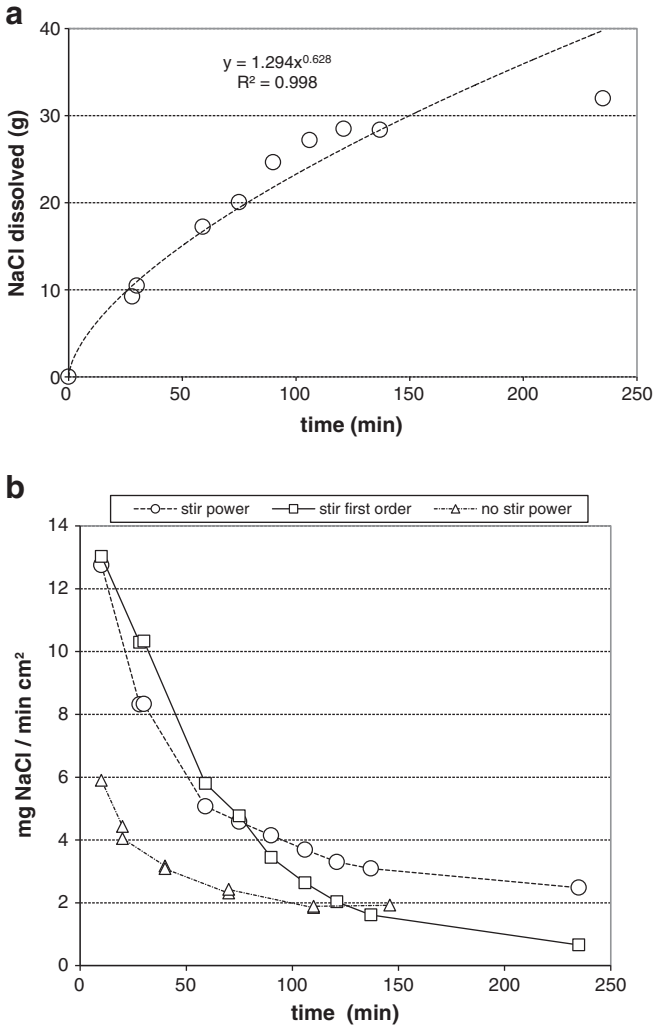

Fig. 5. (a) Power best fit to NaCl dissolution in 50% DS for runs with magnetic stirring. The bars of the analytical error of the data points are too small to be seen on the figure. (b) Comparison of dissolution rates in 50% DS for runs with stirring, calculated by power best fit time derivative (circles) and by first order kinetics (squares, also shown previously in Fig. 4b). Notice the comparison with the slower dissolution rates in 50% DS in runs with *no stirring* (triangles), calculated by the time derivative to the respective power best fit. The latter will be shown again in Fig. 6b and discussed in Section 4.3. Note that the 10 minute points for 50% DS, with and without stirring have been calculated from the respective time derivatives of power best fits.

in Fig. 3a). In contrast to runs with magnetic stirring in which the solution is homogenized throughout the beaker, in the runs with *no stirring* the solution may develop concentration gradients and stratification. This inhomogeneity is due to the dissolution of NaCl which leads to local increase in the density of the brine adjacent to the slice. Although this results in gravitational mixing, that homogenizes the water column, the solution at the top of the beaker remains relatively unaffected, thereby allowing stratification to develop. It should be noted that at the end of each *no stirring* run, stratification that might have built up, is deliberately, completely destroyed by mixing in order to measure precisely the increase in Na and in Cl concentrations which represent the total amount of NaCl that has been dissolved during the run, under the empirical conditions dictated by the experimental set-up. The mixing of the solution does not solve the problem that dissolution might have taken place in a volume that is somewhat smaller than 200 ml. This concern will be further discussed below (Section 4.4). The loss in slice weight measures, in parallel, independently, the amount of dissolved NaCl.

Thus the kinetic model presented above (Section 4.1) which assumes homogenous concentrations in the entire beaker at any time, cannot be applied to the *no stirring* experiments.

The relationship between the amounts of NaCl dissolved and the duration of the *no stirring* runs was assumed to follow a power function. The time derivative of the power function may then yield an estimate of the rate of halite dissolution. This approach was first tested on the set of runs in 50% DS with magnetic stirring (Fig. 5a).

The rates of dissolution derived by the time derivatives of the two methods, first order kinetics and power best fit, are then compared in Fig. 5b and Table 4. These comparisons show that during the first 10 min the rates derived by the two methods are in good agreement and that during the first ~90 min the time derivative of the power fit

Table 4
Momentary dissolution rates of halite at 10 min after run start in 200 ml.

Dissolution rate (mg/cm2 min)			
	No stirring	Stirring 350 rpm	
Method of calculation	Power best fit	First order kinetics	Power best fit
Initial DS dilution			
10% DS	12.2		
50% DS	5.8	13.0	12.8
70% DS	2.8		
90% DS	1.4		

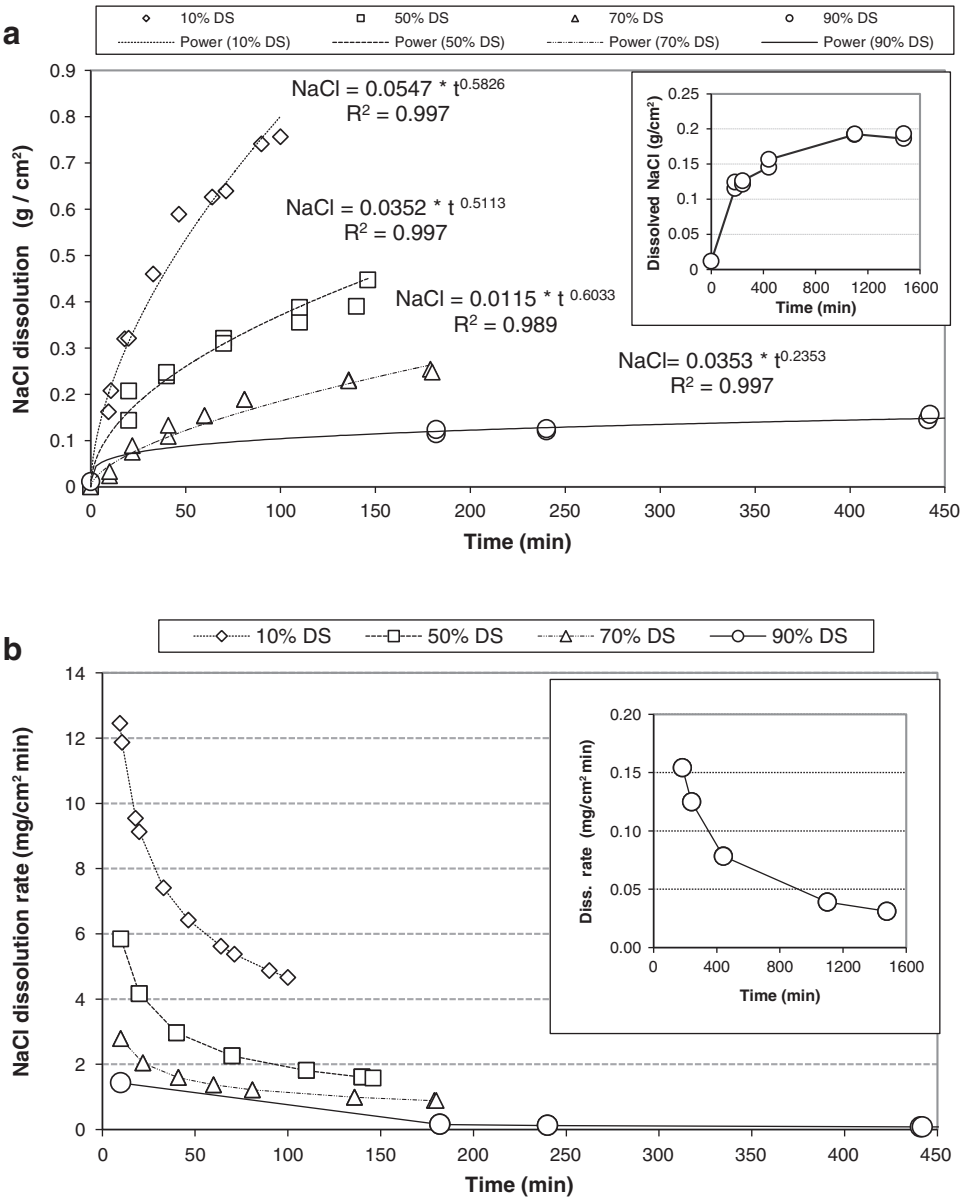

Fig. 6. (a) Runs with no stirring. Power best fits for dissolved NaCl (g), normalized to initial surface area of the slice, in 200 ml DS dilutions to 10%, 50%, 70% and 90%. The data points of >450 min of the 90% DS runs are shown in the insert. (b) Instantaneous rates of halite dissolution in 200 ml DS dilutions, *no stirring*. The data points shown are the dissolution rates occurring at the end of each run, estimated by the time derivatives of the power best fits shown above in Fig. 6a. Rates at >450 min in 90% DS are shown in the insert. Note that the 10 min points for 50% DS and 90% DS have been calculated from the time derivatives of the respective power best fits.

yields dissolution rates which are comparable to the kinetic model. However beyond about 100 min the power derived rates become gradually larger than those estimated by the kinetic model.

Keeping these limitations in mind, the dissolution rates for all the *no stirring* runs were estimated by the power best fit method and are summarized in Fig. 6. The power trend lines between the weights of halite dissolved, normalized to the initial surface area of the slice, and the respective dissolution time, for all the experiments performed in 200 ml of 10%, 50%, 70% and 90% DS dilutions are presented in Fig. 6a. The normalization to surface area was done to minimize the effect of the varying surface areas of the halite slices upon the rate of dissolution. Since at the beginning of each run, at $t = 0$, the halite slice has not yet started to dissolve, a zero data point should be added to the plots. However, it is not possible to apply a power best fit if the data contains a point with coordinates (0,0). Instead, a very close to zero data point, (0.001; 0.001) was used and then slightly changed until a best fit (highest R^2) was achieved. The power best fits for the *no stirring* runs, which are shown in Fig. 6a are based on the W data. Very similar best fits were obtained with the W_{Na} and W_{Cl} data.

The instantaneous rate of dissolution at the end of each run calculated for all the data points of the power best fits (Fig. 6a) by the respective time derivatives are presented in Fig. 6b.

4.3. Comparison of halite dissolution rates

It can be seen in Fig. 6b, that the degree of dilution influences not only the dissolution potential but also the rate of dissolution: the highest rates of dissolution achieved in 10% DS dilution are faster by about one order of magnitude than in the 90% DS dilution. Also note that with *no stirring*, in 50% DS the dissolution rate is about twice slower than with stirring (Fig. 5b).

Fig. 6b shows, as has already been seen in the runs with stirring (Fig. 4b), also in the runs with *no stirring* the dissolution rates of halite do decrease with time. This feature is in accordance with the decreasing

instantaneous dissolution potential, since, the brine concentration increases with time during the run. The relationship between dissolution rate and brine concentration is discussed hereafter in Section 4.4.

At 10 min with stirring the power derivative method yields an estimate of halite dissolution rate which is in good agreement with the rate derived by the kinetic model (Table 4). Also given in Table 4 are the rates at 10 min without stirring in the DS dilutions. It can be readily seen that there is an inverse linear correlation between the degree of the DS dilution and the dissolution rates of halite that is brought in contact with these dilutions. This seems to be important because it may help to predict the initial dissolution rates of sub-surface halite deposits when brought in contact with more and more diluted solutions as the level of the freshwater–brine interface is continuously declining.

Dissolution rates in the Dead Sea solutions were compared with those reported in pure NaCl solutions that have been measured (Alkattan et al., 1997a) in an experimental set-up that is not very different from the one used in this study. For instance, in a 50% DS dilution at 10 min, with 350 rpm stirring, the dissolution rate was 13 mg/cm2 min and the salinity of the solution (TDS) at 10 min was 174 g/l. At this same salinity but in a pure NaCl solution, the dissolution rate estimated from Alkattan et al. (1997a) data, at 270 rpm, is 43 mg/cm^2 min, which is 3 times more fast than in the DS dilution. Similar comparisons also at other salinities yield the same result, about threefold faster rates in pure NaCl solutions than in the DS dilutions. These differing rates might be due to several causes, which may lead to a combined effect.

(a) There is semblance between the experimental set-ups, but they are not identical. For instance, it could be that the surface area of disks with compressed NaCl powder (Alkattan et al., 1997a) is effectively larger than the surface of polished halite slices of the same size.
(b) The methods of calculating the dissolution rate are different.
(c) The lower dissolution rates in the Dead Sea solutions vs. the pure NaCl solutions might be related to the low solubility of NaCl in DS (Gavrieli et al., 1989) in the presence of the very high concentrations of Mg and of Ca (2.2 and 0.5 m, respectively; Table 1) and to the very low water activity in DS brines (Krumgalz, 1997). For instance, in the DS brine of December 2004 (Table 1) the water activity was 0.66.

The above mentioned comparison stresses the importance of measuring dissolution rates of halite in natural solutions, because they might be different than those in pure NaCl solutions.

4.4. Approach to saturation and its relationship to the rate of halite dissolution

At the end of each run the filtrate (see above Section 2.1) was submitted to complete chemical analysis. The analytical results, i.e. the detailed chemical composition of the solution, were used to calculate the degree of halite saturation (DSH) at the run end with the PHREEQC program. Also calculated by this program were the expected Na concentrations in each DS dilution if brought to halite saturation by NaCl addition (i.e. to DSH = 1; see Table 3). Fig. 7 displays the measured concentrations of Na at the end of each run, expressed as Na molalities (mole Na/kg water) vs. the respective calculated DSH value. Also shown are the Na molalities for each dilution if brought to DSH = 1. The Figure clearly illustrates that each initial DS dilution follows a distinct pathway, the dissolution potential of that particular dilution that gradually approaches halite saturation,

Unlike most of the figures shown above, where dissolution was given as a function of time, Fig.7 shows, regardless of run duration, the amounts of NaCl that can be dissolved in a certain DS dilution. Obviously, the larger the initial DS dilution, the larger is the amount of NaCl that can be dissolved in this solution. This increased NaCl solubility with increasing DS dilution, might also be due to respective lower Ca and Mg concentrations.

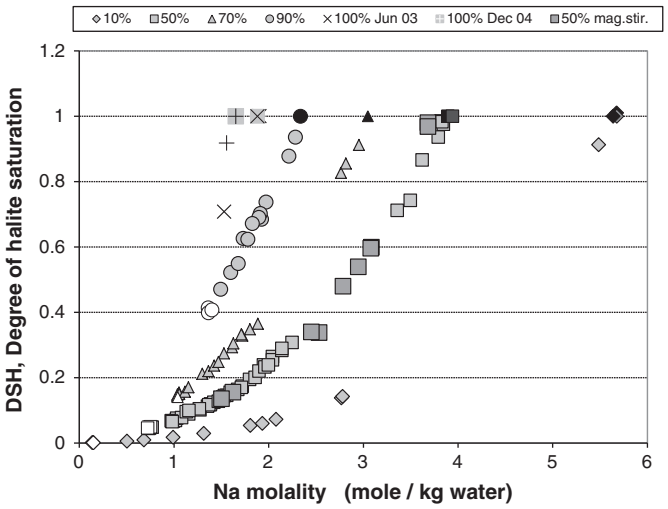

Fig. 7. Na molalities vs. the degree of halite saturation, DSH. Initial dilutions are marked by empty symbols, runs at their end and runs for saturation attainment by light colored symbols. The calculated Na molalities at DSH = 1 are shown in dark, full-colored symbols. Also shown are the Na molalities vs. DSH of the undiluted DS (100% DS) from June 2003 (symbol×) and from December 2004 (symbol+) as well as the respective calculated Na molalities at DSH = 1 (respective shadowed symbols).

Finally, Fig.7 also reveals that for 10%, 50% and 70% DS dilutions, at the beginning of their respective pathways, relatively large NaCl dissolution (i.e. Na additions) do not cause a dramatic increase in DSH. Only in the 90% DS dilution, relatively small Na additions have a larger effect on the DSH, causing a sharper DSH increase already at the initial stage of the pathway.

Fig. 6b (see above) has shown previously that in all the DS dilutions, the dissolution rate in runs with no stirring decreases as the run duration becomes longer. While the dissolution rate decreases, the solution gradually becomes more concentrated in NaCl and gradually approaches saturation with respect to halite. This relationship is shown in Fig. 8 where the DSH values that prevail at the end of each non-stirring run are plotted vs. the respective dissolution rates. The general, evident trend in Fig.8 is that as DSH's increase the dissolution rates decrease, (see also insert for the 90% DS runs) emphasizing that the DSH is in fact dictating the dissolution rate. Moreover the data points of all the DS dilutions converge into a common coherent trend. A practical outcome of this observation would be that, by defining the DSH of a certain DS solution, the initial rate of NaCl dissolution in it under no-stirring conditions, can be predicted.

It should be noted that for runs with no stirring the DSH calculations have been based on measured concentrations of major ions in the 200 ml solution at the end of each run. But, if the dissolution proceeds mainly in the volume next to the halite slice which, being denser mixes with the volume below, then halite dissolution takes place in about 160 ml instead of 200 ml. If this volume could be analyzed separately, somewhat larger concentrations of Na and Cl will be obtained at the run end leading to larger DSH values. Calculations show (Appendix 1) that at the faster dissolution rates that take place at relatively low DSH values, the consequence of the diminished, effective dissolution volume (to 160 ml) is minor: a slight increase in DSH, by <0.08 units. Only at slow dissolution rates, below 1 mg/cm^2 min, where larger DSH values prevail, if the dissolution takes place in a volume of only 160 ml, the increase of the DSH becomes more meaningful, between 0.08 and 0.16 DSH units. The DSH values calculated for the non-stirring runs in 200 ml, should therefore be regarded as minimal values, but the general trend of the dissolution rate–DSH relationship shown in Fig. 8 remains very much the same.

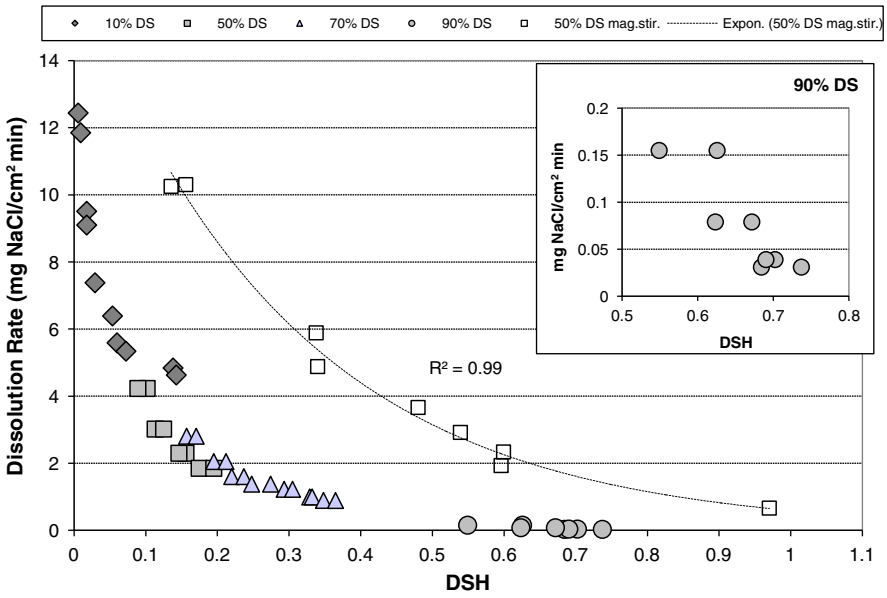

Fig. 8. Degree of halite saturation vs. dissolution rate of halite at end of runs with no stirring in DS dilutions of 10% (rhombes), 50% (squares), 70% (triangles) and 90% (circles). Runs with magnetic stirring in 50% DS dilution are also shown (empty squares).

The data points of DSH vs. dissolution rate for runs with magnetic stirring at an initial 50% DS dilution are also presented in Fig. 8 (empty squares). The clear inverse relationship between DSH and the dissolution rate can be readily seen. Fig.8 also emphasizes that regardless of reaction duration at any DSH value of a solution, the dissolution rate with stirring is faster than with no-stirring. Also, because dissolution with perpetual stirring represents in fact the upper limit of dissolution rate in a certain DS dilution, the curved, concave shape of the DSH vs. dissolution rate shown by these runs could be of general use for estimating halite interaction with DS dilutions.

4.5. The relevance of the derived halite dissolution potentials and dissolution rates to the DS environment

(a) At the subsurface, where undersaturated groundwaters with a large range of salinities (10% to 90% DS) are found (Yechieli et al., 2006; Abelson et al., 2006), similar to the dilutions used in this study, dissolution of halite is an ongoing process, provided groundwater flow is fast enough. A preliminary study assessing the rate of formation of sinkholes by ground-water-fed dissolution was done by Shalev et al. (2006) who used a low dissolution rate (1.2 mg/cm^2 min). The range of dissolution rates obtained in the present study (up to 13 mg/cm^2 min), suggests that sinkhole formation might be faster than previously estimated by Shalev et al. (2006). The very recent detailed study of the Zeelim Dead Sea Coast (Avni et al., 2015) demonstrates that in addition to sinkhole formation due to the relatively slow halite dissolution by groundwater flow, the accumulation of floodwaters in sinkholes induces fast dissolution in shallow depth halite layers and accelerates new sinkholes formation. Since floodwaters are fresh water, (unlike ground waters which are Dead Sea dilutions), it is reasonable that they will produce much faster dissolution rates, as also suggested by the comparisons of dissolution rates vs. dilution degree given above.

Without flow, which is somewhat similar with the no-stirring experiments saturation in the vicinity of the halite layer will be achieved and dissolution will be retarded. On the other hand, the experiments with stirring simulate better the field situation where groundwater flow is significant. The real situation in the field varies in the different locations and probably is somewhere between the two extreme cases of fast flow and no flow at all.

(b) The DS surface layer, when diluted by floodwater dissolves halite from the lake floor in shallow areas and from the delta of the end brine (Beyth et al., 1998). A possible application of the present study is the estimate of the rates and quantities of halite that can be dissolved from these areas by rising DS lake levels in winters of high rainfall.

Also, if and when a Red Sea-Dead Sea canal will become operative, the DS lake level will rise and the more diluted upper layer of the Dead Sea that will be formed will dissolve halite deposits from shallow lake floor and shoreline areas in large quantities that can be now forecasted with the dissolution potential data given in this study.

5. Summary and conclusions

1. Halite dissolution experiments carried out with stirring ensured homogenous solutions throughout the run duration while in those carried out with no stirring, some stratification developed, hindering the dissolution. The 'real' situation is probably somewhere in-between the two extremes of our experimental set-up, depending on the environmental conditions (e.g. rate of groundwater flow).

The present set of experiments shows that in quiescent conditions the initial dissolution rates of halite in Dead Sea dilutions (10% to 90% DS; 32.5 to 290 g TDS/l, respectively), are inversely related to the initial salinity of the solution, the higher the salinity the slower the dissolution rate. The rates at 10 min decrease linearly (Table 4), from 12.2 mg/cm^{2-} min in 10% DS to 1.4 mg/cm^2 min in 90% DS. In experiments performed under constant stirring conditions with 50% DS, the dissolution rates were about twice as fast as with 50% DS in quiescent conditions.

2. In stirred runs at 10 min, the dissolution rate of halite in a DS dilution is threefold slower than in a pure NaCl solution (Alkattan et al., 1997a) of similar salinity: 13 mg/cm^2 min vs. 42 mg/cm^2 min at a TDS concentration of 174 g/l. This threefold ratio was maintained also at all other TDS concentrations that have been compared.
3. This study presents, for the first time in natural solutions such as the dilutions of the Dead Sea brine, the clear dependence of halite

dissolution rates upon the degree of halite saturation, DSH. The rates are exponentially decreasing faster in runs with no stirring and in both types of runs the exponential decrease is faster as the DSH approaches saturation.

4. Measurements of solution densities and of solution volumes at the end of the experiments enabled to quantify the increase in density and the concomitant increase in volume following dissolution of 1 g NaCl per liter which are 0.00057 g/cm^3 and 0.074 ml/l, respectively, regardless of the initial DS dilution.
5. The wide range of DS dilutions, from 10% to 90%, the varying ratios of solution volume to halite surface area and the comparison (at 50% DS) between stirring and no-stirring conditions enables us to predict dissolution rates of halite, within a reasonable limit, for a wide range of salinities and limiting flow conditions.

Acknowledgements

We thank Dr. Vladimir Lyakhovsky for mathematical advice, Dr. Rotem Golan and Peter Rendel for computational advice, Dina Stiber, Dr. Olga Yoffe and Dr. Sara Ehrlich for the chemical analyses. Robert Knafo, Shlomo Ashkenazy and Chaim Hemo are acknowledged for technical help. The study was supported by project no. 40388 of the Israeli Ministry of National Infrastructure.

Appendix 1

DSH, degree of halite saturation, vs. dissolution rate: comparison between DSH values shown in Fig.8 (squares dissolution in 200 ml) with calculated DSH values if dissolution of halite took place in only in only 160 ml (rhombes).

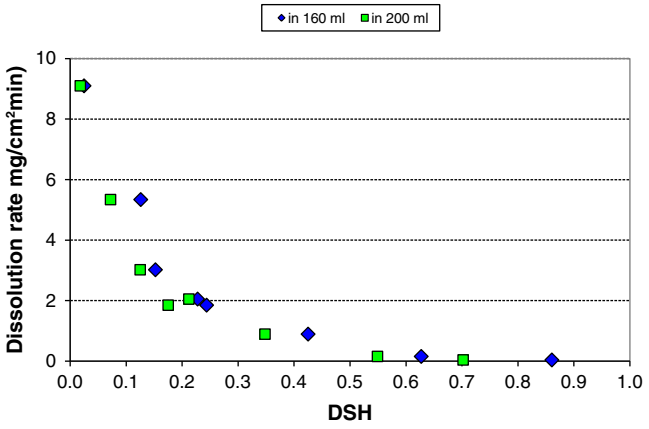

References

Anati, D.A., Gavrieli, I., Oren, A., 1995. The residual effect of the 1991-1993 rainy winters on the Dead Sea stratification. Isr. J. Earth Sci. 44, 63–70.

Abelson, M., Yechieli, Y., Crouvi, O., Baer, G., Wachs, D., Bein, A., Shtivelman, V., 2006. Evolution of the Dead Sea sinkholes. In: Enzel, Y., Agnon, A., Stein, M. (Eds.), New Frontiers in Dead Sea Paleoenvironmental Research. Geological Society of America, pp. 241–253 (Special Paper).

Alkattan, M., Oelkers, E.H., Dandurand, J.L., Schott, J., 1997a. Experimental studies of halite dissolution kinetics 1, the effect of saturation state and the presence of trace metals. Chem. Geol. 137, 201–219.

Alkattan, M., Oelkers, E.H., Dandurand, J.L., Schott, J., 1997b. Experimental studies of halite dissolution kinetics: II. The effect of the presence of aqueous trace anions and K3Fe(CN)6. Chem. Geol. 143, 17–26.

Avni, Y., Lensky, N., Dente, E., Shviro, M., Arav, R., Gavrieli, I., Yechieli, Y., Abelson, M., Lutzky, H., Filin, S., Haviv, I., Baer, G., 2015. Self-accelerated development of salt karst during flash floods along the Dead Sea Coast, Israel. J. Geophys. Res. Earth Surf. 121:17–38. http://dx.doi.org/10.1002/2015JF003738.

Beyth, M., Katz, O., Gavrieli, I., 1998. Propagation and retrogradation of the Salt Delta in the Southern Dead Sea: 1985–1992. Isr. J. Earth Sci. 46, 95–106.

Dijk, P.E., Berkowitz, B., Yechieli, Y., 2002. Measurement and analysis of dissolution patterns in rock fractures. Water Resour. Res. 38 (2). http://dx.doi.org/10.1029/2001Wr000246.

Durie, R.W., Jessen, F.W., 1964a. Mechanism of the dissolution of salt in the formation of underground salt cavities. Soc. Pet. Eng. J. 4 (2):183–190. http://dx.doi.org/10.2118/678-PA (Trans. AIME, 231 SPE-678-PA).

Durie, R.W., Jessen, F.W., 1964b. The influence of surface features in the salt dissolution process. Soc. Pet. Eng. J. 4 (3):275–281. http://dx.doi.org/10.2118/1005-PA (Trans AIME 231, SPE_1005-PA).

Field, L.P., Palumbo-Roe, B., Milodowski, A.E., Hall, M.R., Parke, D., Evans, D., 2015. Dissolution experiments in halite cores: comparisons in cavity shapes and controls between brine and seawater experiments. 25th Anniversary Goldschmidt Conference, Prague, August 16–21, 2015, p. 894 (Abstract).

Gertman, I., Hecht, A., 2002. The Dead Sea hydrography from 1992 to 2000. J. Mar. Syst. 35, 169–181.

Gavrieli, I., Starinsky, A., Bein, A., 1989. The solubility of halite as a function of temperature in the highly saline Dead Sea brine system. Limnol. Oceanogr. 34 (7), 1224–1234.

Gavrieli, I., Ben-Avraham, Z., Gat, J.R., 1997. Halite deposition from the Dead Sea 1960–1993. In: Niemi, T. (Ed.), The Dead Sea: the Lake and its Setting. Oxford University Press, pp. 161–170 (chap. 14).

Gavrieli, I., Oren, A., 2004. The Dead Sea as a dying lake. In: Nihoul, J.C.J., Zavialo, P., Micklin, P. (Eds.), Dying and Dead Seas; Climatic Versus Anthropogenic CausesNATO ARW/ASI Series. Kluwer Academic Pub.

Herut, B., Gavrieli, I., Halicz, L., 1998. Coprecipitation of trace and minor elements in modern authigenic halite from the hypersaline Dead Sea brine. Geochim. Cosmochim. Acta 62 (9), 1587–1598.

Krumgalz, B., 1997. Ion interaction approach to geochemical aspects of the Dead Sea. In: Niemi, T.M., Ben-Avraham, Z., Gat, J.R. (Eds.), The Dead Sea, the Lake and its Setting, pp. 145–160 (Chap. 13).

Lensky, N.G., Dvorkin, Y., Lyakhovsky, V., Gertman, I., Gavrieli, I., 2005. Water, salt and energy balances of the Dead Sea. Water Resour. Res. 41, W12418. http://dx.doi.org/10.1029/2005WR004084.

Oz, I., Shalev, E., Yechieli, Y., Gavrieli, I., Levanon, E., Gvirtzman, H., 2016. Salt dissolution and sinkhole formation. J. Geophys. Res. Earth Surf. http://dx.doi.org/10.1002/2016JF003902.

Pilcher, R.S., Blumstein, R.D., 2007. Brine volume and salt dissolution rates in Orca Basin, northeast Gulf of Mexico. AAPG Bull. 91 (5):823–833. http://dx.doi.org/10.1306/12180606049.

Parkhurst, D.L., Appelo, C.A.J., 2013. Description of input and examples for PHREEQC version 3 – a computer program for speciation, batch-reaction, one-dimensional transport, and inverse geochemical calculations. Modeling and Techniques. In: U.S. Geol. Surv. Tech. Methods vol. 6. U.S. Geological Survey, Denver, Colorado.

Starinsky, A., 1974. Relationship Between Ca-chloride Brines and Sedimentary Rocks in Israel. Ph.D. thesis. The Hebrew University, Jerusalem (176 p. (in Hebrew)).

Shalev, E., Lyakhovsky, V., Yechieli, Y., 2006. Salt dissolution and sinkhole formation along the Dead Sea shore. J. Geophys. Res.:111 http://dx.doi.org/10.1029/2005JB004038.

Steinhorn, I., 1983. In–situ salt precipitation at the Dead Sea. Limnol. Oceanogr. 28, 580–583.

Stiller, M., Gat, J.R., Bauman, N., Shasha, S., 1984. A meromictic episode in the Dead Sea: 1979–1982. Verh. Int. Ver. Theor. Angew. Limnol. 22, 132–135.

Stiller, M., Sigg, L., 1990. Heavy metals in the Dead Sea and their co-precipitation with halite. Hydrobiologia 197, 83–89.

Stiller, M., Gat, J.R., Kaushansky, P., 1997. Halite precipitation and sediment deposition as measured in sediment traps deployed in the Dead Sea: 1981–1983. In: Niemi, T.M., Ben-Avraham, Z., Gat, J.R. (Eds.), The Dead Sea: The Lake and its Setting. Oxford University Press, pp. 184–192.

Stiller, M., Yechieli, Y., Gavrieli, I., 2007. The rate of dissolution of halite in diluted Dead Sea brines. Report GSI/01/2007 (19 p., 3 Tables and 11 Figures).

Wachs, D., Yechieli, Y., Stivelman, V., Itamar, A., Baer, G., Goldman, M., Raz, E., Riebekov, M., Shatner, U., 2000. Formation of Sinkholes along the Shore of the Dead Sea– Summary of Finding from the First Stage of Research: Geological Survey Report GSI/41/2000 (in Hebrew), 49 p.).

Wagner, C.J., 1949. The dissolution rate of sodium chloride with diffusion and natural convection as rate-determining factors. J. Phys. Chem. 53 (7):1030–1033. http://dx.doi.org/10.1021/j150472a005.

Weisbrod, N., Alon-Mordish, C., Konen, E., Yechieli, Y., 2012. Dynamic dissolution of halite rock during flow of diluted saline solutions Geophys. Res. Lett. 39 (L09404):2012. http://dx.doi.org/10.1029/2012GL051306.

Yechieli, Y., Abelson, M., Bein, A., Crouvi, O., Shtivelman, V., 2006. Sinkholes "swarms" along the Dead Sea coast: Reflection of disturbance of lake and adjacent groundwater systems. GSA Bull. 118, 1075–1087.

Zak, I., 1967. Mount Sdom. (Ph.D. thesis). Hebrew university, Jerusalem.

Zidane, A., Zechner, E., Huggenberger, P., Younes, A., 2014. Simulation of rock salt dissolution and its impact on land subsidence. Hydrol. Earth Syst. Sci. 18:2177–2189. http://dx.doi.org/10.5194/hees-18-2177-2014.